RM L9K14a

NACA

RESEARCH MEMORANDUM

TANK TESTS AT SUBCAVITATION SPEEDS OF AN ASPECT-RATIO-10 HYDROFOIL WITH A SINGLE STRUT

By Kenneth L. Wadlin, John A. Ramsen,
and John R. McGehee

Langley Aeronautical Laboratory
Langley Air Force Base, Va.

NATIONAL ADVISORY COMMITTEE
FOR AERONAUTICS

WASHINGTON

July 20, 1950
Declassified May 20, 1953

NATIONAL ADVISORY COMMITTEE FOR AERONAUTICS

RESEARCH MEMORANDUM

TANK TESTS AT SUBCAVITATION SPEEDS OF AN ASPECT-RATIO-10 HYDROFOIL WITH A SINGLE STRUT

By Kenneth L. Wadlin, John A. Ramsen, and John R. McGehee

SUMMARY

An investigation was made in Langley tank no. 2 to determine the lift and drag characteristics of a rectangular hydrofoil with an aspect ratio of 10 supported by a single strut. The model was tested at various depths below the water surface at speeds up to 35 feet per second corresponding to a Reynolds number of 2.0×10^6.

A maximum lift-drag ratio of 25.4 was obtained with the hydrofoil at a depth of 1/2 chord. This ratio decreased and the lift coefficient at which it occurred increased with depth. The effects of the water surface were negligible at a depth of 2 chords or greater. The data at a Reynolds number of 2.0×10^6 showed good agreement with corresponding aerodynamic data from wind-tunnel tests.

INTRODUCTION

An investigation is being conducted in Langley tank no. 2 of the lift-drag ratios of hydrofoil-strut combinations applicable to the design of high-speed water-borne craft. As the first phase of the investigation it appeared desirable to determine experimentally, at subcavitation speeds and various depths of submersion, the lift and drag of a high-aspect-ratio rectangular hydrofoil supported by a single strut and having an airfoil section. This phase was of interest to determine whether lift-drag ratios in the order of 20 were attainable with a structurally feasible system and to determine how the lift and drag characteristics of the hydrofoil as predicted from aerodynamic data are affected by depth of submersion and the free water surface.

The measurements were made at water speeds from 15 to 35 feet per second. The size of the model was chosen to give a Reynolds number of 2.0×10^6 at 35 feet per second.

DESCRIPTION OF MODEL

The model (see fig. 1) consisted of an 8-inch-chord hydrofoil with an aspect ratio of 10 supported by an 8-inch-chord strut intersecting the upper surface of the hydrofoil without fillets. The strut was perpendicular to the chord line of the hydrofoil. The foil and strut were made of stainless steel with a yield strength of 100,000 pounds per square inch. They were polished to a smooth finish consistent with current wind-tunnel practice.

The hydrofoil had an NACA 64_1A412 section which differs from the NACA 64_1-412 section only by removal of the trailing-edge cusp. The section characteristics are essentially the same. (See reference 1.) The strut had an NACA 66_1-012 section. Figure 2 gives the sections and ordinates for the foil and the strut as computed from references 1 and 2.

The 64-series section was chosen since it is designed for a moderate extent of laminar flow. The results would therefore be more nearly applicable at high values of the Reynolds number, say in the order of 20.0×10^6, than if sections having a larger extent of design laminar flow had been used. (See reference 3.) The design lift coefficient of 0.4 was chosen since preliminary calculations based on data in reference 2 indicated that the maximum lift-drag ratio would occur near this lift coefficient. A thickness of 12 percent was chosen as a compromise between the increasing strength and increasing minimum drag coefficient with increasing thickness ratio.

The 66-series section was chosen for the strut (see fig. 1) since its small frontal angle is more suitable for intersecting the water surface than the larger frontal angles for the sections with the minimum pressure farther forward. The 12-percent thickness was chosen as the minimum thought to be structurally adequate.

APPARATUS AND PROCEDURE

The tests were made using the main carriage of Langley tank no. 2. Figure 3 shows a view of the test setup with the hydrofoil and balance attached to the support structure on the carriage.

The hydrofoil was moved vertically by means of a motor-driven jacking screw which moved the balance and hydrofoil system as a unit. Change of angle of attack was obtained at the plate attaching the strut to the balance. One end of the plate was pivoted while the other end

was moved with another jacking screw to obtain the desired angle. Over the range of angles of attack tested, the change in depth caused by change in angle was negligible.

Measurements of lift and drag were made by means of electrical strain gages. The force measurements were made at constant speed, angle of attack, and depth of submersion. The depth of submersion is defined as the distance from the water surface to the point on the foil nearest the water surface. A range of submersions from 3.5 inches (0.44 chord) to 30.0 inches (3.75 chords), and speeds from 15 to 35 feet per second were covered. At each speed the angle of attack was increased from 0° until the peak in lift-drag ratio was obtained. The lift and drag forces caused a negligible change in angle of attack.

The supporting strut was run alone at the same range of speeds, depths, and angles as the combination. For these tests the end of the strut was fitted with a faired cap.

The forces obtained were converted to the usual aerodynamic lift and drag coefficients using a value of ρ of 1.966 slugs per cubic foot corresponding to a water temperature during the tests of 70° F. All coefficients were based on the area of the hydrofoil, 4.44 square feet.

The drag coefficients were corrected for the ground effect of the bottom of the tank (see reference 4) by using the equation

$$(C_D)_{corrected} = (C_D)_{measured} + \delta\frac{C_L^2}{\pi R}$$

where R is the aspect ratio, and δ is an interference coefficient that varies with the distance from the hydrofoil to the tank bottom. Values of δ from reference 4 used for the various depths are given in figure 4.

A similar ground-effect correction was applied to the angle of attack by the equation

$$\alpha_{corrected} = \alpha_{measured} + \delta\frac{C_L}{\pi R}$$

where α is measured in radians.

RESULTS AND DISCUSSION

The uncorrected data for the complete model (hydrofoil and strut) are presented in figures 5 and 6 as plots, for each depth, of lift coefficient and drag coefficient, respectively, against speed with angle of attack as a parameter. For a given depth, the lift coefficient did not vary appreciably with speed over the range tested. The drag coefficient did not vary appreciably with speed from 25 to 35 feet per second though it did increase at lower speeds. Both lift coefficient and drag coefficient increased with increasing depth over the range tested. The variation of lift coefficient at depths greater than 2 chords, however, was negligible.

The strut drag data are presented in figure 7(a) as a plot of drag coefficient against speed with depth as a parameter. The strut drag coefficient was small compared to the total drag coefficient and did not vary with speed. Figure 7(b) is a plot of drag coefficient against depth.

The faired curves of figures 5 to 7 were obtained by cross fairing the data. These cross fairings were used to obtain values at depths of 0.5, 1.0, 2.0, 3.0, and 3.5 chords which were used in the computations of all subsequent plots.

The variations of lift–drag ratio (corrected for ground effect) with lift coefficient and depth of submersion are shown in figure 8. Since lift coefficient did not vary with speed and drag coefficient was constant above 25 feet per second, figure 8(b) is typical for speeds from 25 to 35 feet per second. The variations in lift–drag ratio at the two speed conditions are similar in character. The maximum values obtained were 23.2 at 15 feet per second and 25.4 at 35 feet per second.

At depths of 2 chords or greater the lift–drag ratio values decreased in a regular manner with increasing depth at all values of lift coefficient. This results from the fact that below a depth of 2 chords, the forces on the hydrofoil were not varying appreciably with depth, the lift–drag ratio of the combination being reduced principally by the increase in strut drag with depth.

At depths less than 2 chords the lift–drag ratio varied in the same manner as at the greater depths until the peak was reached.

Figure 9 shows the variation, with depth and speed, of the maximum lift–drag ratio and the lift coefficient at which the maximum lift–drag ratio occurred. It can be seen that as the depth increased, the maximum

lift–drag ratio decreased and the lift coefficient at which the maximum lift–drag ratio occurred increased. This is to be expected since the strut drag increases with depth.

Figure 10 is a plot of the data at a speed of 35 feet per second (Reynolds number of 2.04×10^6) after subtracting the strut tares given in figure 7, making corrections for ground effect and converting the coefficients to infinite aspect ratio by the usual equations. These equations are

$$C_{D_i} = \frac{C_L^2}{\pi R}(1 + \sigma)$$

$$\alpha_i = \frac{C_L}{\pi R}(1 + \tau)$$

where σ and τ are corrections for rectangular wings dependent on aspect ratio. For an aspect ratio of 10, the value of σ is 0.088; the value of τ is 0.25. Also included in figure 10 are the aerodynamic data at a Reynolds number of 2.0×10^6 for the NACA 64_1–412 section as given in reference 5. The slope of the lift curve and the lift coefficient for a given angle of attack increased with increasing depth. At depths of 2 chords and greater the agreement with the aerodynamic data is good. The drag coefficients fall between the aerodynamic data for the smooth condition and the standard roughness condition. The variation due to depth was very small compared to the possible effects due to roughness. During the tests the surface of the model was slightly pitted by the salt water in the tank and was probably rougher than in the aerodynamic tests. This surface condition may have significant effects from practical considerations but unfortunately no data were taken to show these effects.

Because of the large aspect ratio and the agreement with the aerodynamic data it appears that any interference effects of the strut are small. Since interference increases with increasing lift coefficient, it is possible that if an interference correction could be made the slopes of the drag curves would agree even better.

The results of the investigation should not be considered to apply at higher absolute speeds than those tested since cavitation, which is a function of the absolute speed, greatly affects the characteristics of hydrofoil systems.

CONCLUDING REMARKS

The results of the tank tests of the hydrofoil–strut combination may be summarized as follows:

1. A maximum lift–drag ratio of 25.4 was obtained with the hydrofoil at a depth of 1/2 chord below the surface.

2. The maximum lift–drag ratio decreased and the lift coefficient at which it occurred increased with depth principally because of the increasing drag of the strut.

3. The water surface had a negligible effect on the lift and drag characteristics of the hydrofoil at depths of 2 chords or greater.

4. The hydrofoil lift and drag characteristics obtained at a Reynolds number of 2.0×10^6 showed good agreement with aerodynamic data at the same Reynolds number.

Langley Aeronautical Laboratory
National Advisory Committee for Aeronautics
Langley Air Force Base, Va.

REFERENCES

1. Loftin, Laurence K., Jr.: Theoretical and Experimental Data for a Number of NACA 6A-Series Airfoil Sections. NACA Rep. 903, 1948. (Formerly NACA TN 1368, 1947.)

2. Abbott, Ira H., Von Doenhoff, Albert E., and Stivers, Louis S., Jr.: Summary of Airfoil Data. NACA Rep. 824, 1945.

3. Braslow, Albert L., and Visconti, Fioravante: Investigation of Boundary-Layer Reynolds Number for Transition on an NACA $65_{(215)}$-114 Airfoil in the Langley Two-Dimensional Low-Turbulence Pressure Tunnel. NACA TN 1704, 1948.

4. Reid, Elliott G.: Applied Wing Theory. First Ed., McGraw-Hill Book Co., Inc., 1932, pp. 166-176.

5. Loftin, Laurence K., Jr., and Smith, Hamilton A.: Aerodynamic Characteristics of 15 NACA Airfoil Sections at Seven Reynolds Numbers from 0.7×10^6 to 9.0×10^6. NACA TN 1945, 1949.

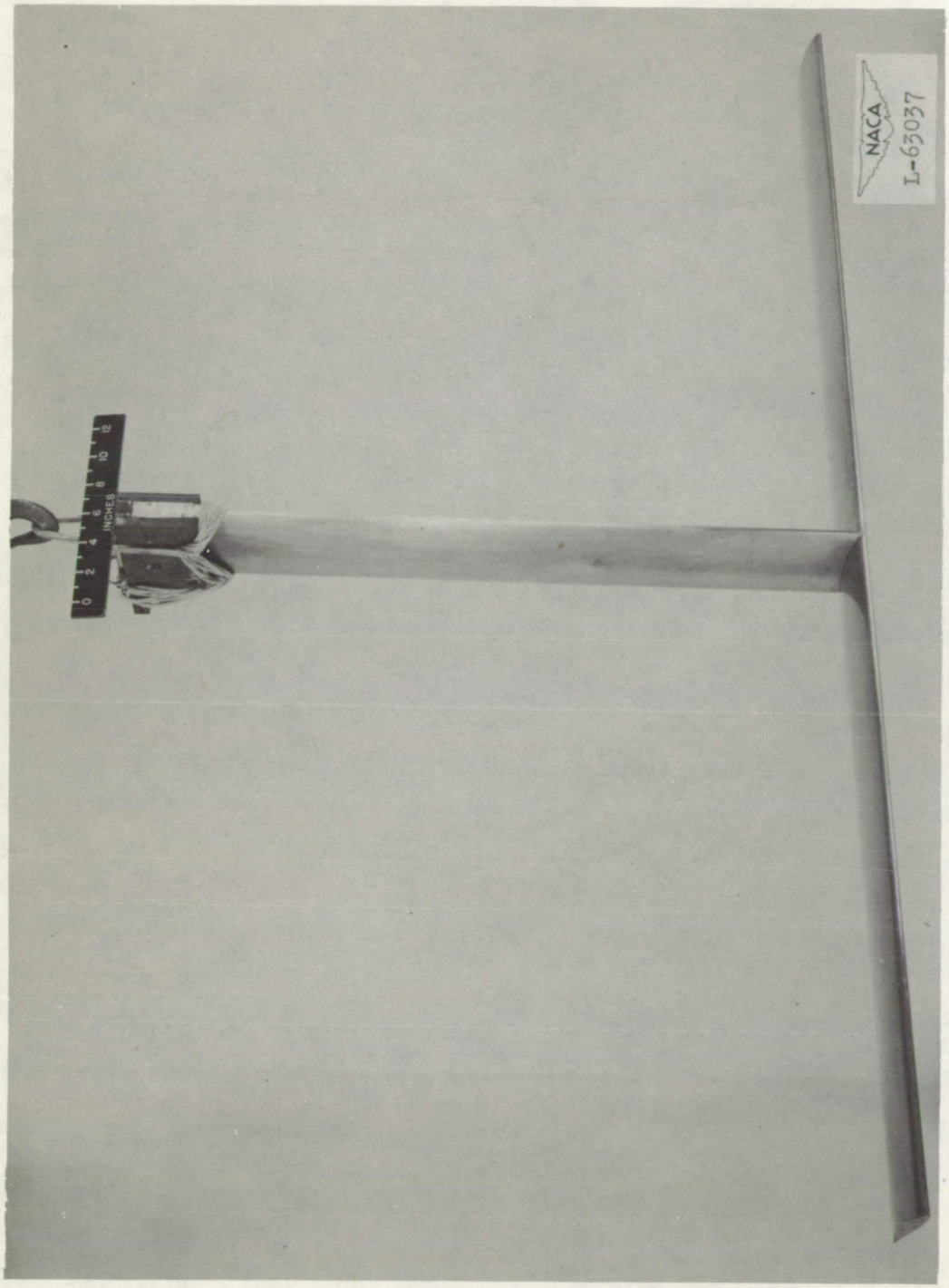

Figure 1.- Photograph of strut and hydrofoil.

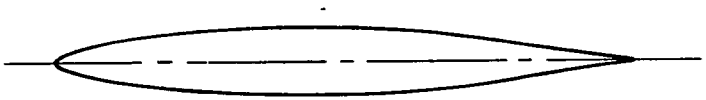

Strut, NACA 66_1-012

Station	Ordinate
0	0
.040	.072
.060	.087
.100	.109
.200	.145
.400	.200
.600	.243
.800	.280
1.200	.339
1.600	.384
2.000	.419
2.400	.445
2.800	.464
3.200	.476
3.600	.480
4.000	.477
4.400	.467
4.800	.447
5.200	.411
5.600	.361
6.000	.301
6.400	.236
6.800	.167
7.200	.099
7.600	.038
8.000	0

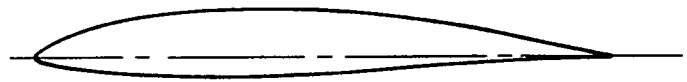

Hydrofoil, NACA 64_1A412

Upper surface		Lower surface	
Station	Ordinate	Station	Ordinate
0.026	0.084	0.054	-0.067
.044	.104	.076	-.079
.082	.135	.118	-.096
.178	.194	.221	-.126
.376	.279	.424	-.164
.575	.346	.625	-.190
.790	.401	.810	-.211
1.176	.490	1.224	-.241
1.578	.559	1.622	-.261
1.981	.611	2.019	-.274
2.384	.648	2.416	-.281
2.788	.673	2.812	-.281
3.192	.684	3.208	-.275
3.595	.679	3.605	-.259
3.999	.661	4.001	-.236
4.398	.632	4.402	-.207
4.795	.592	4.805	-.176
5.192	.544	5.208	-.142
5.590	.487	5.610	-.108
5.988	.422	6.012	-.076
6.386	.349	6.414	-.050
6.786	.265	6.814	-.034
7.190	.179	7.210	-.022
7.595	.090	7.605	-.012
8.000	.002	8.000	-.002

Figure 2.- Sections and ordinates of strut and hydrofoil.

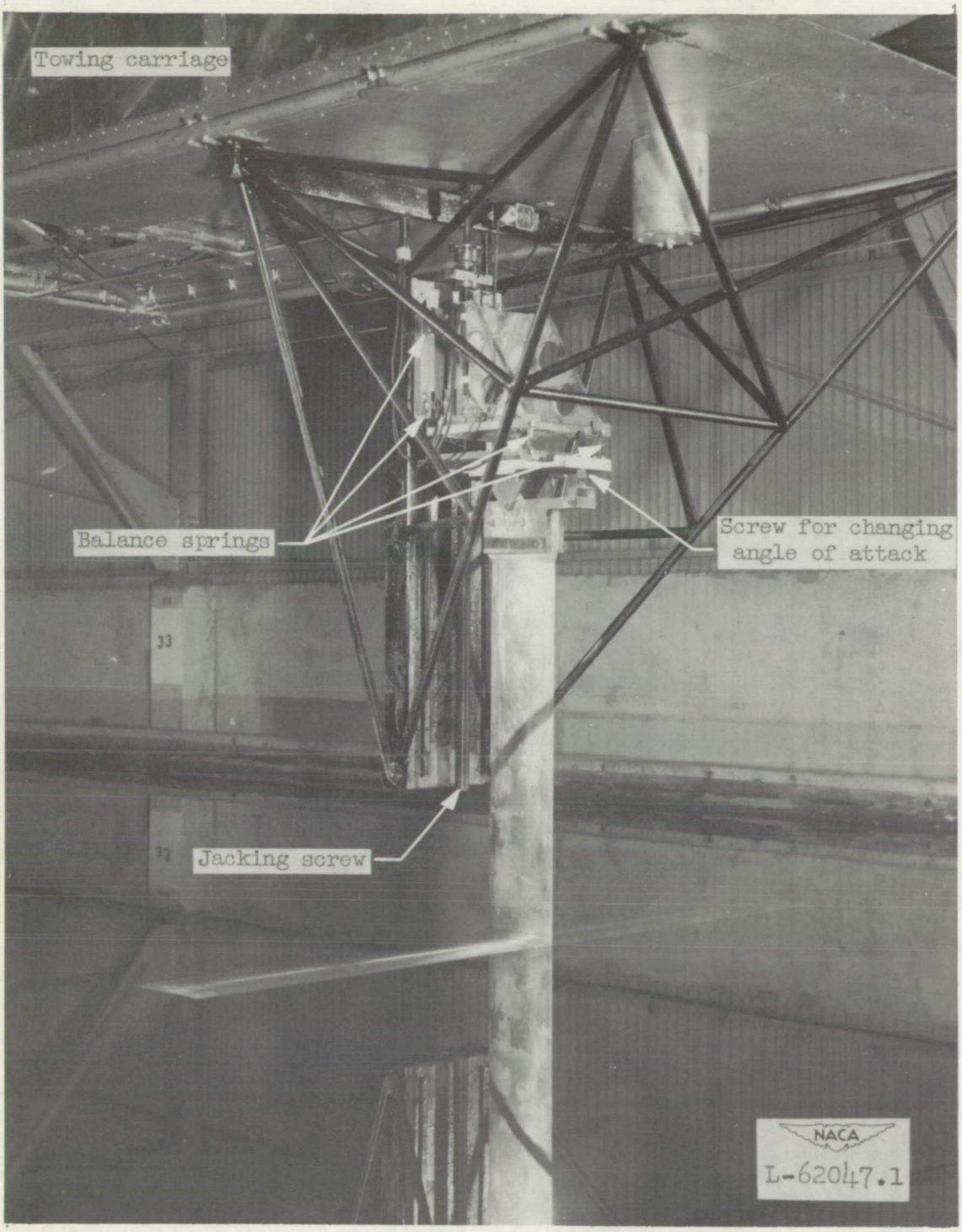

Figure 3.- Test setup showing aspect-ratio-10 hydrofoil and balance attached to towing carriage.

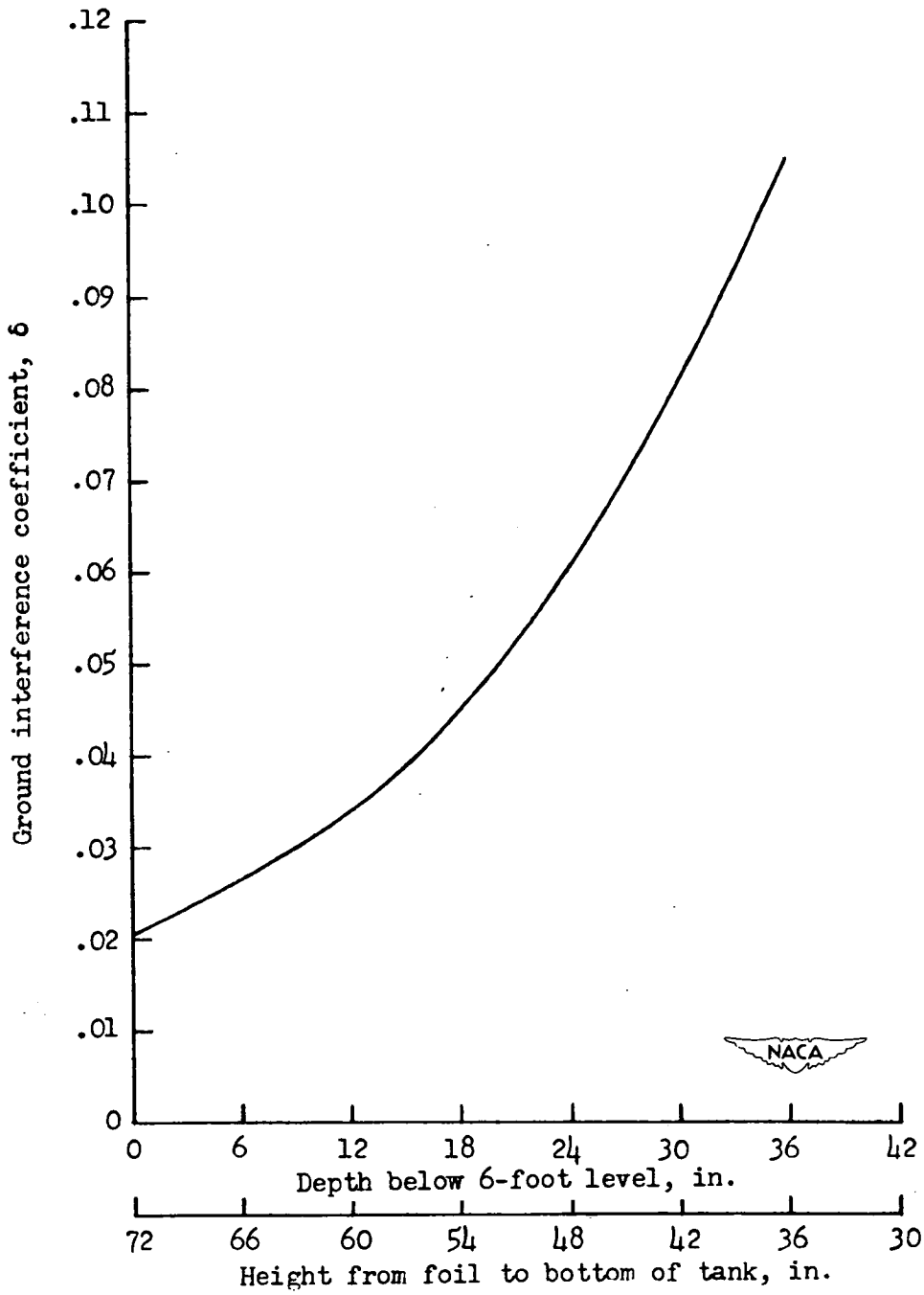

Figure 4.- Variation of ground interference coefficient δ with depth.

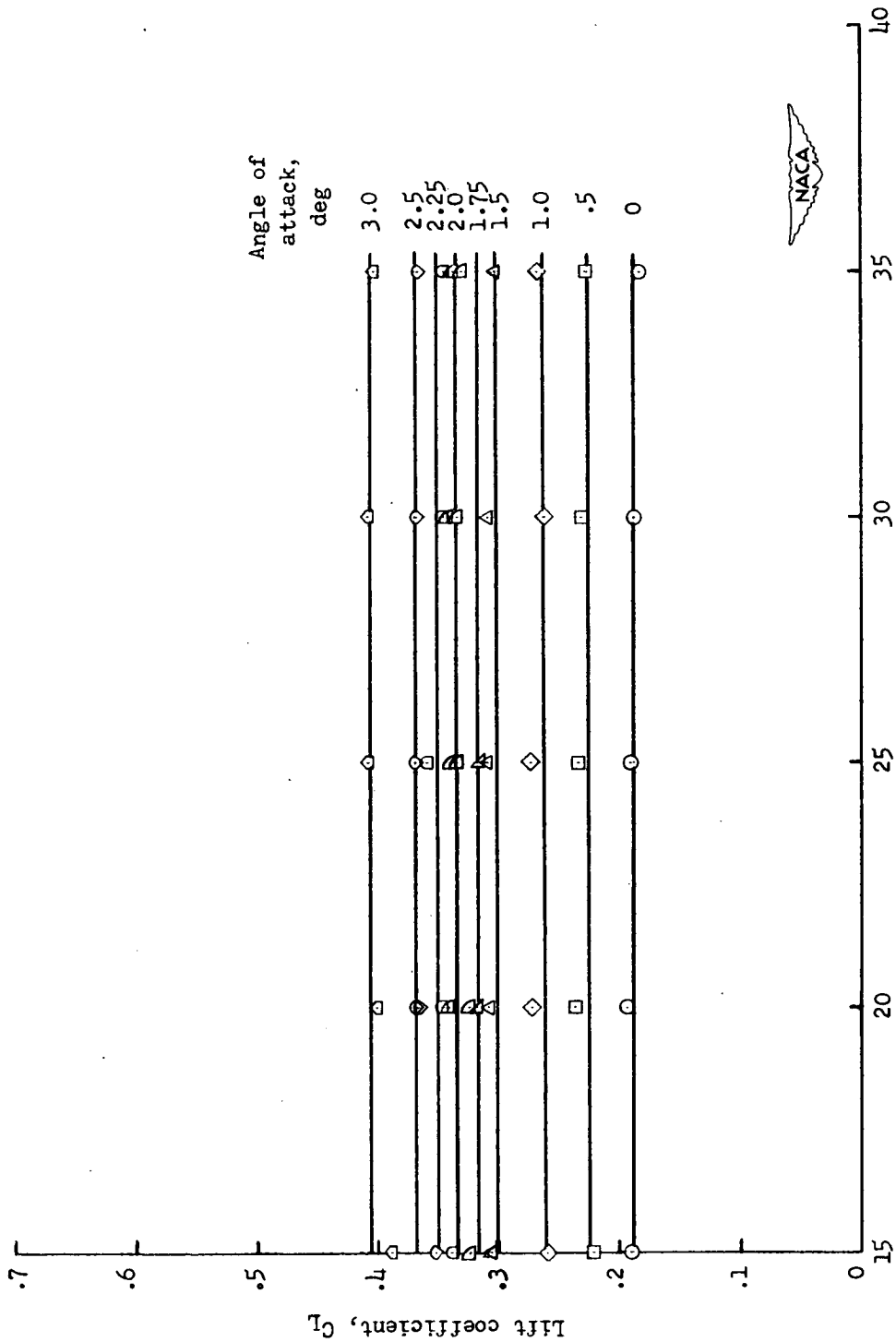

(a) 3.5-inch depth.

Figure 5.- Uncorrected data - variation of lift coefficient with speed for hydrofoil-strut configuration.

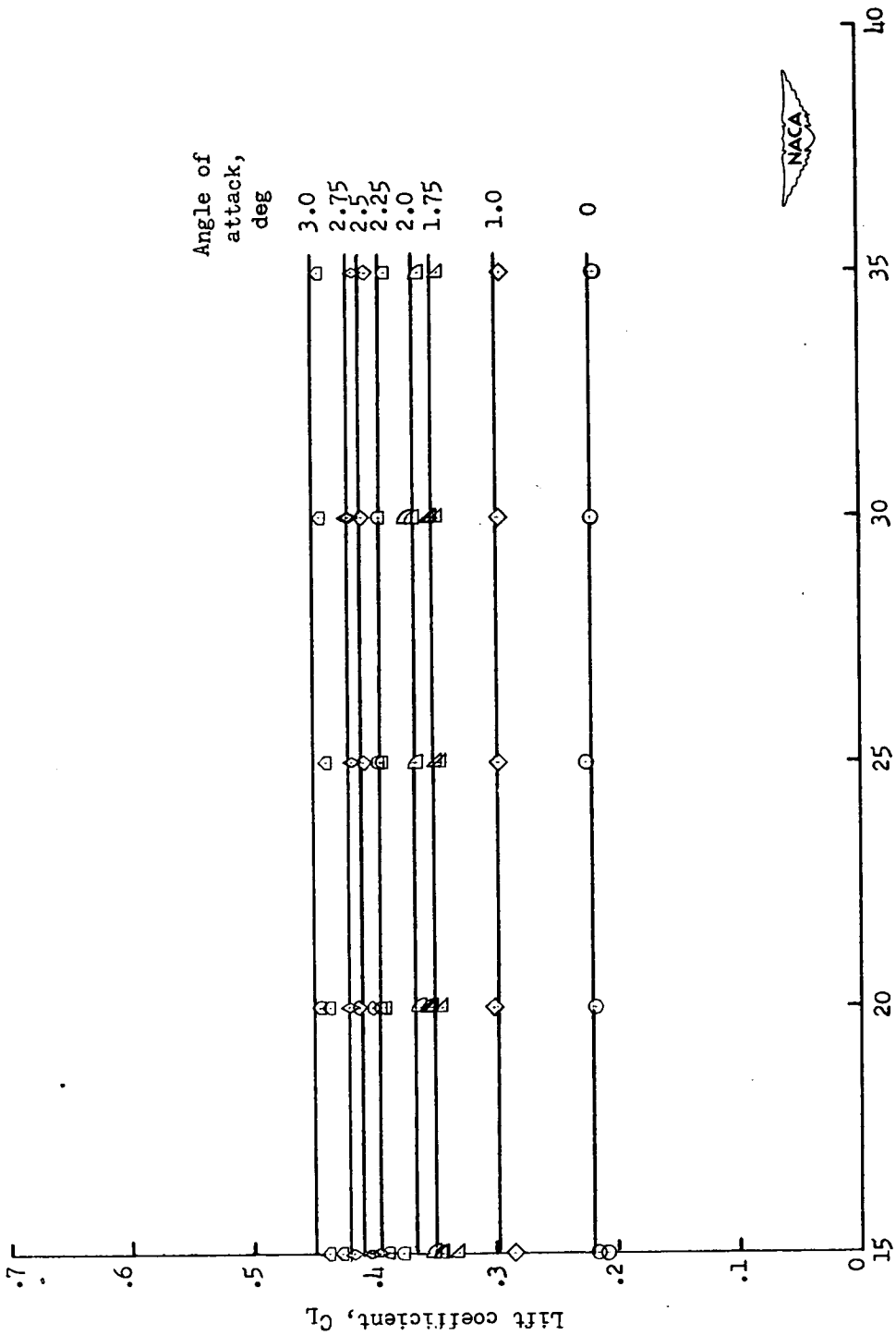

(b) 6.0-inch depth.

Figure 5.- Continued.

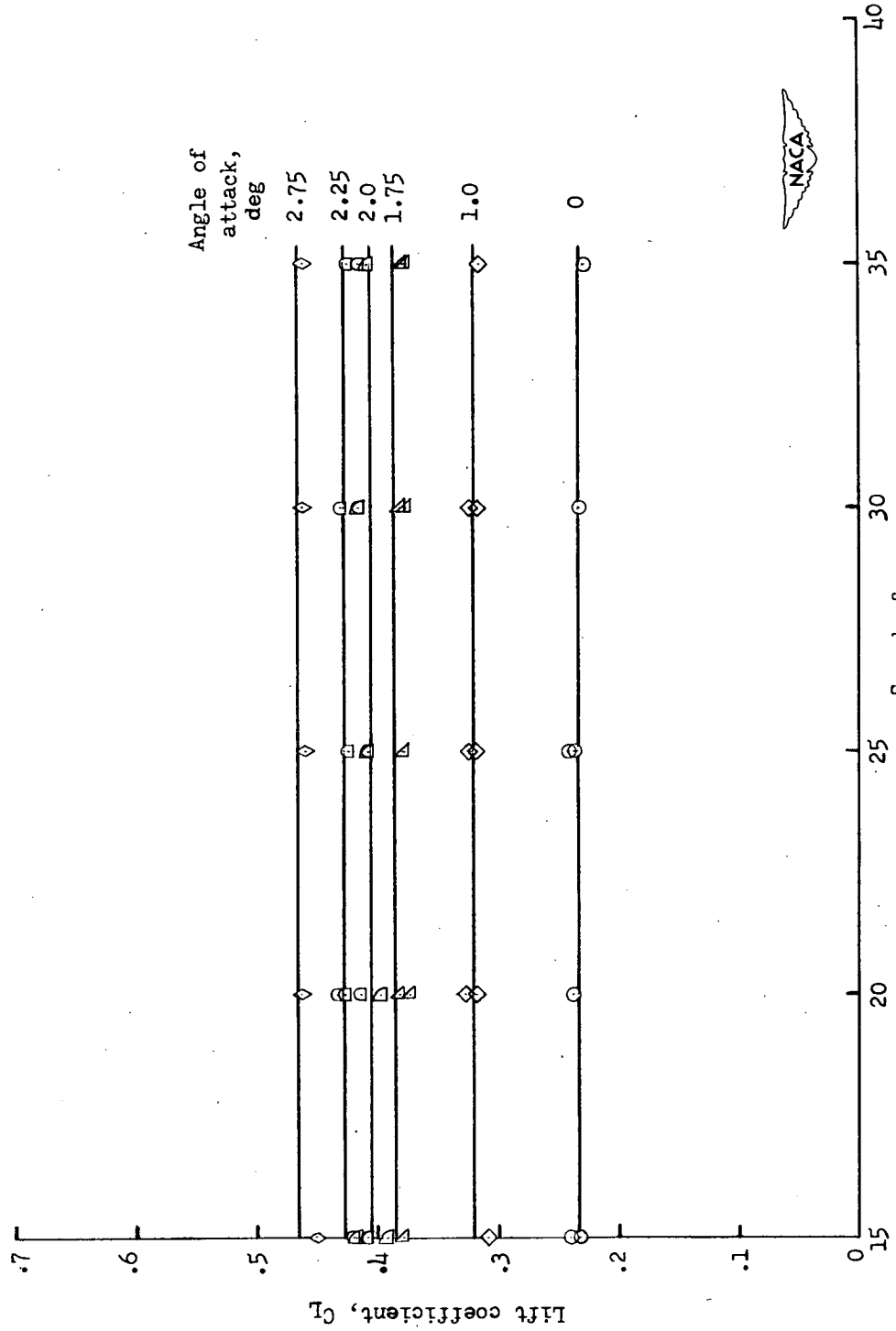

(c) 12.0-inch depth.

Figure 5.- Continued.

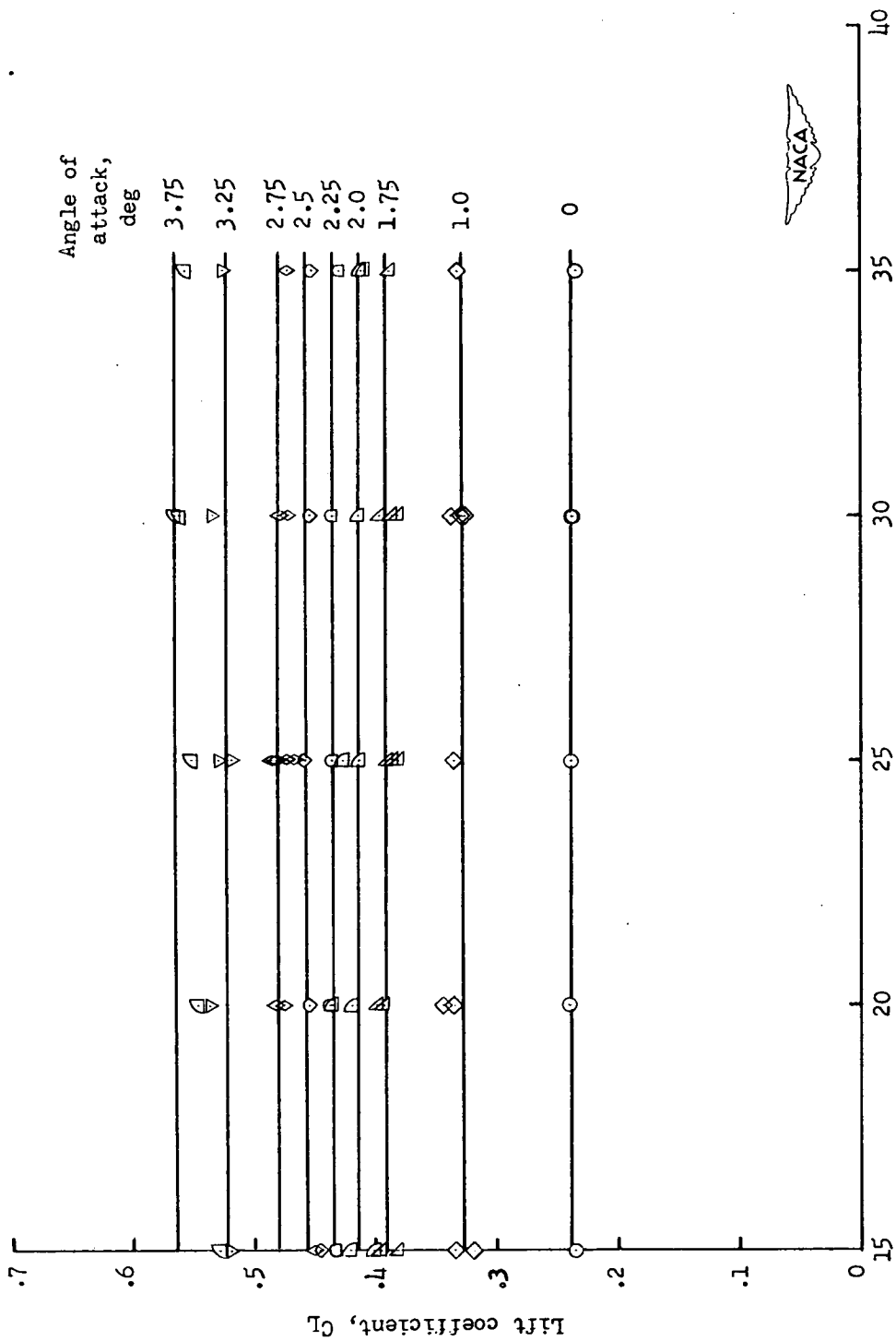

(a) 18.0-inch depth.

Figure 5.- Continued.

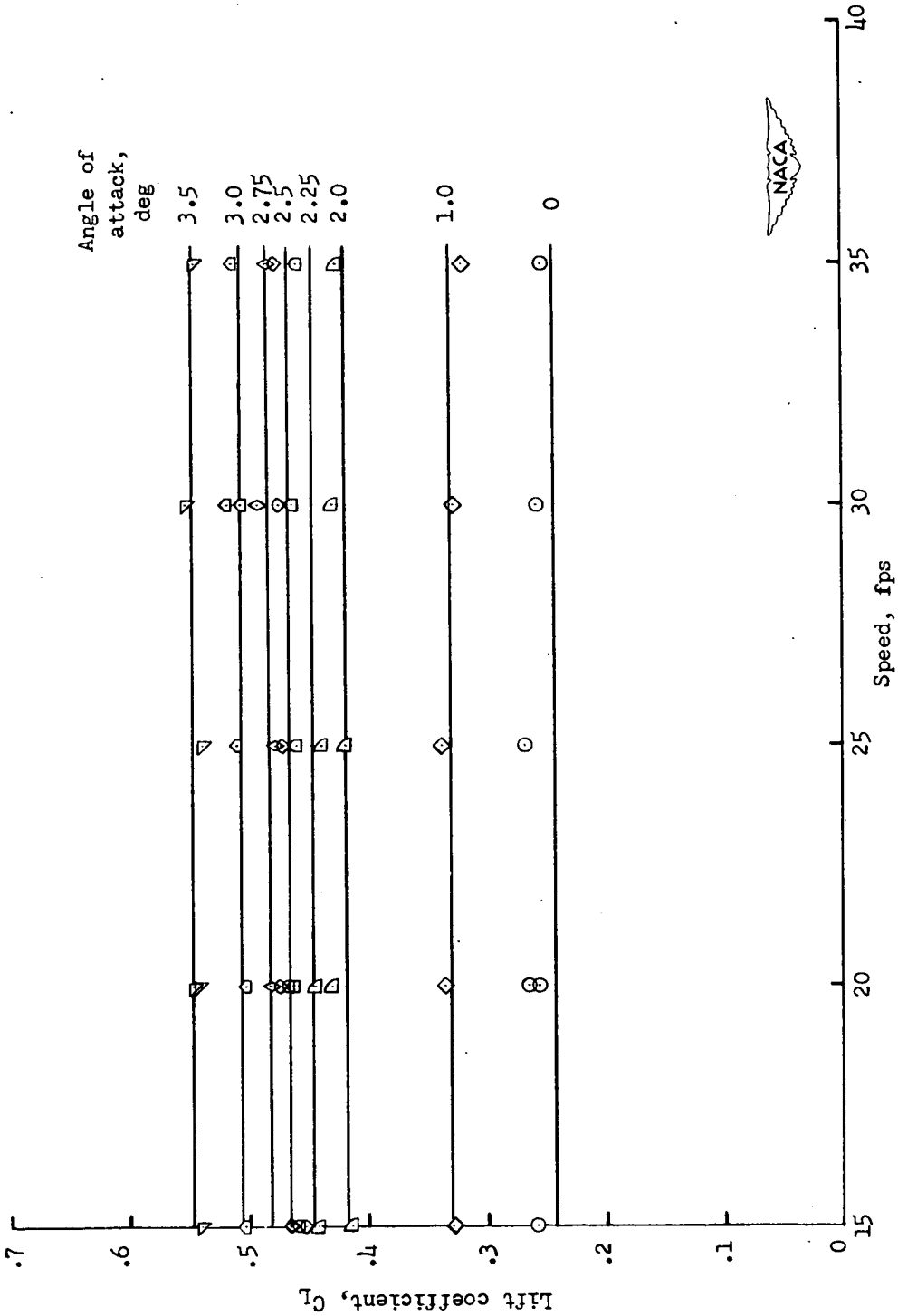

(e) 24.0-inch depth.

Figure 5.- Continued.

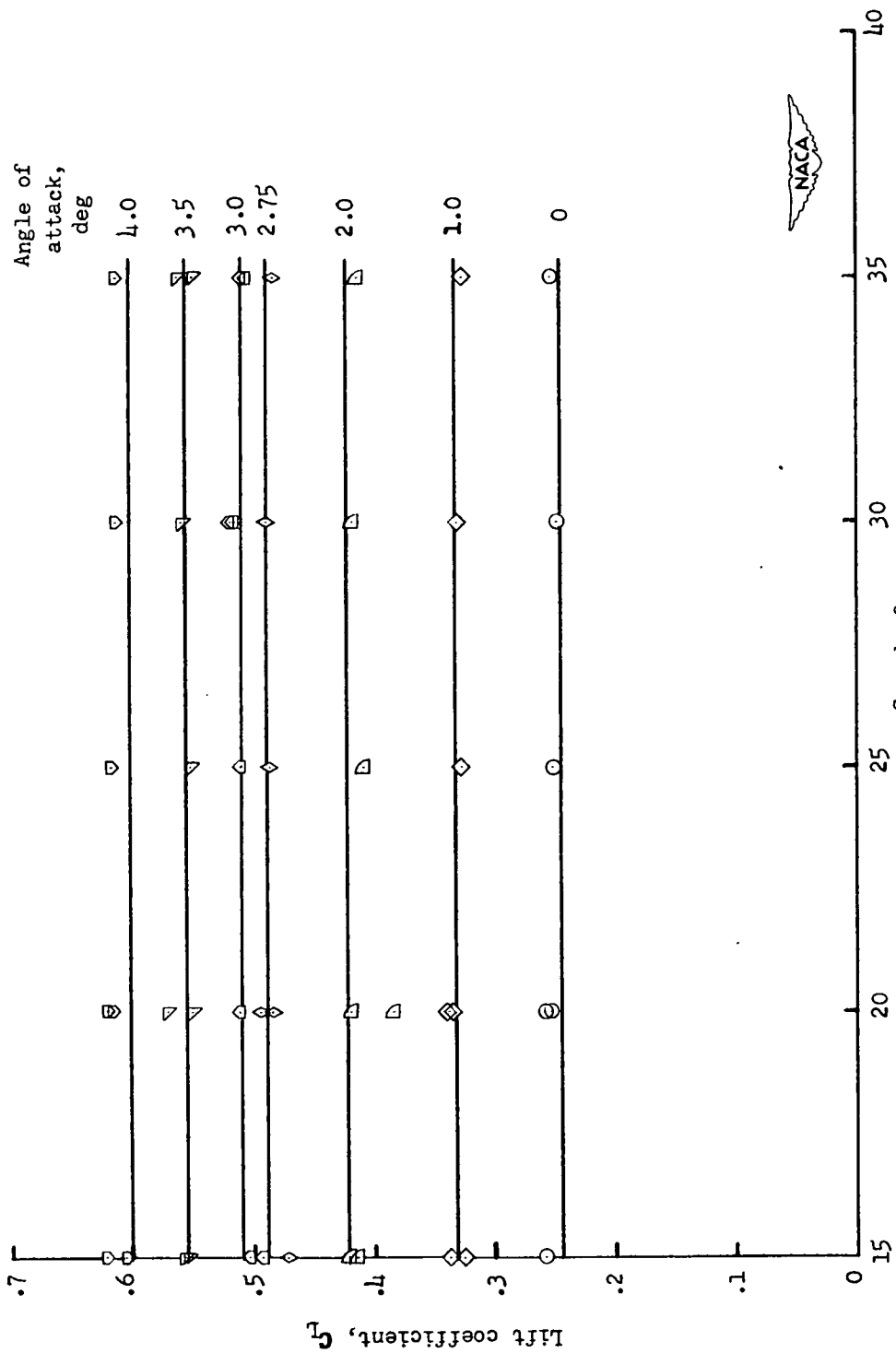

(f) 30.0-inch depth.

Figure 5.- Concluded.

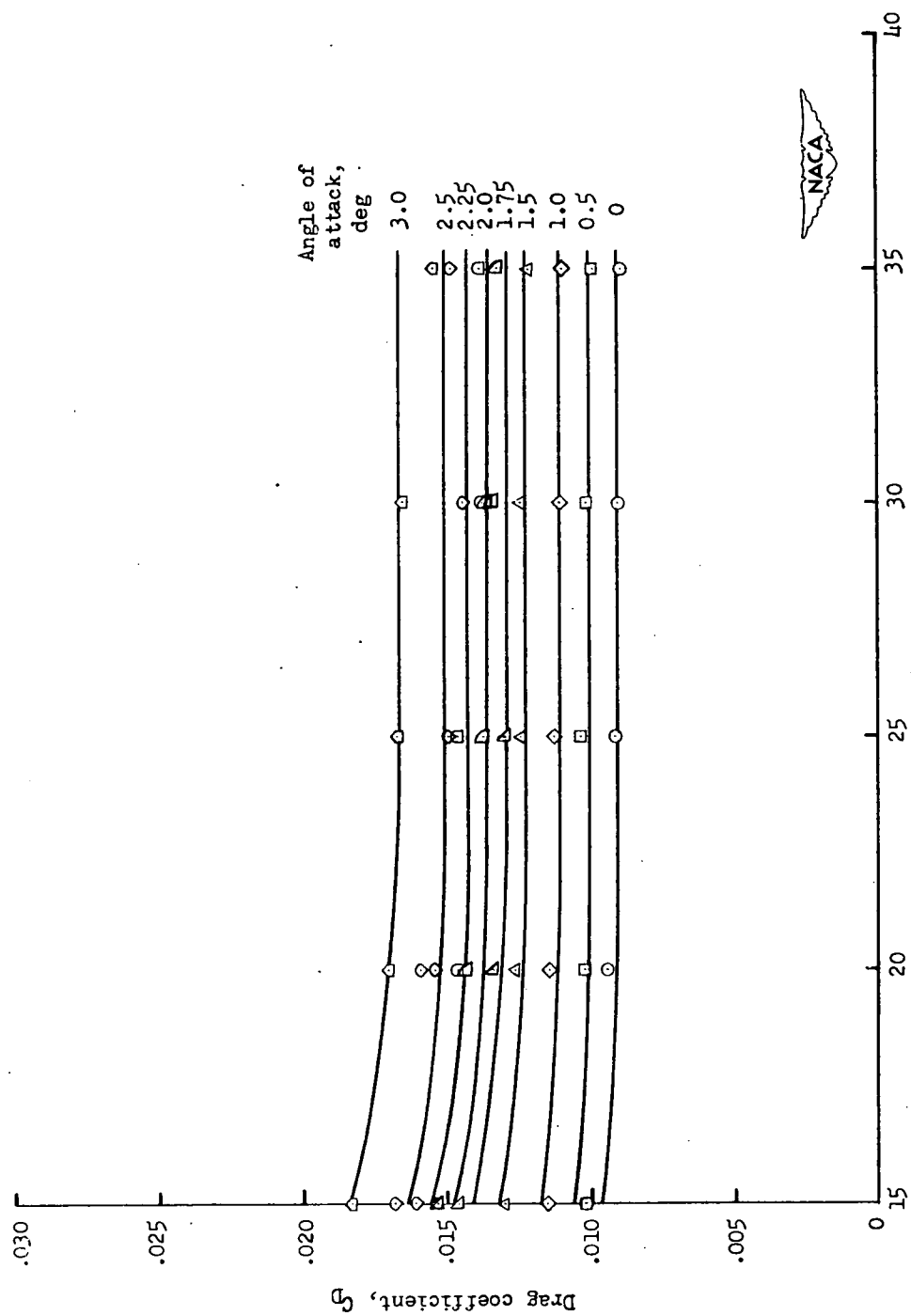

(a) 3.5-inch depth.

Figure 6.- Uncorrected data - variation of total drag coefficient of hydrofoil-strut configuration with speed.

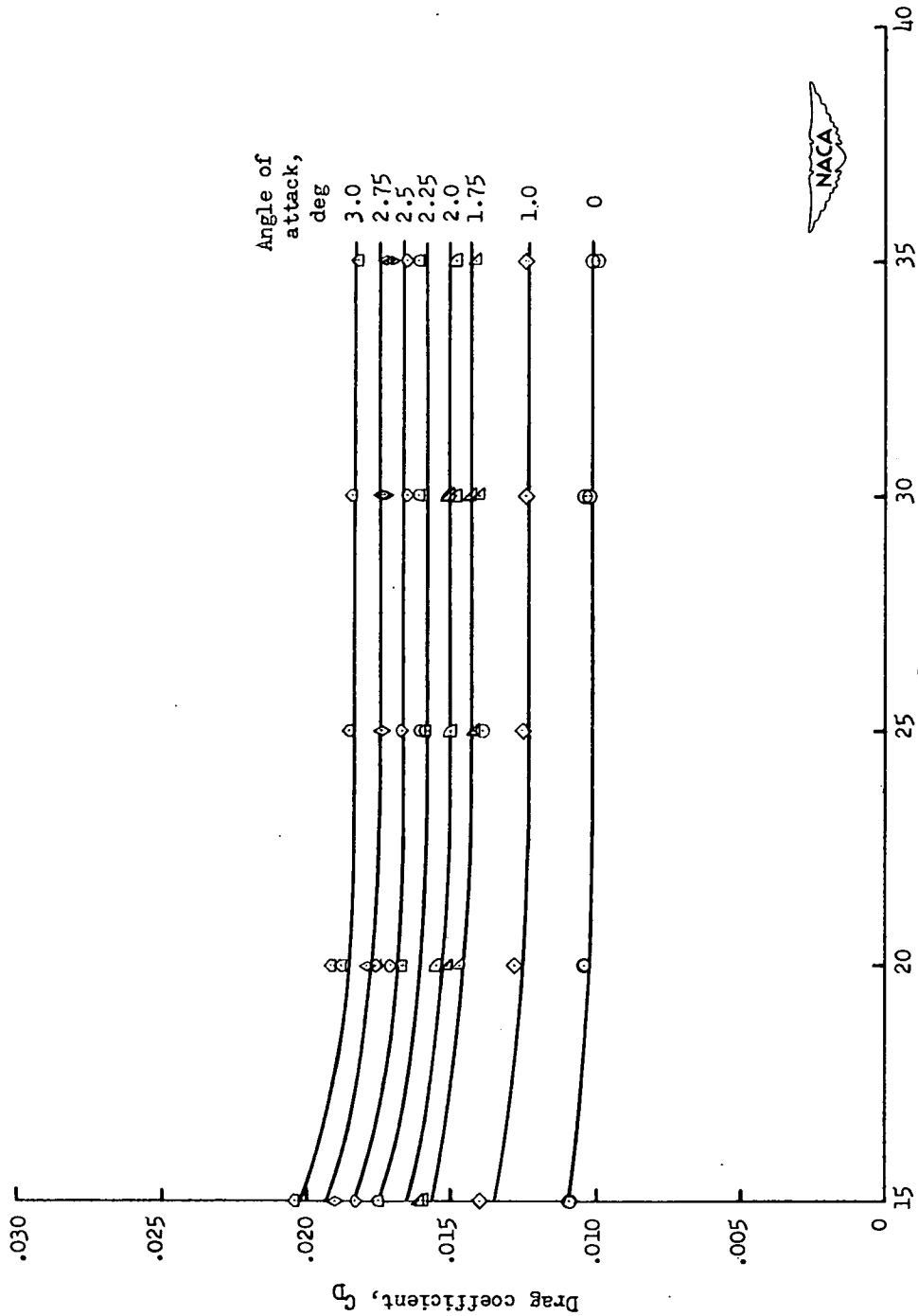

(b) 6.0-inch depth.

Figure 6.- Continued.

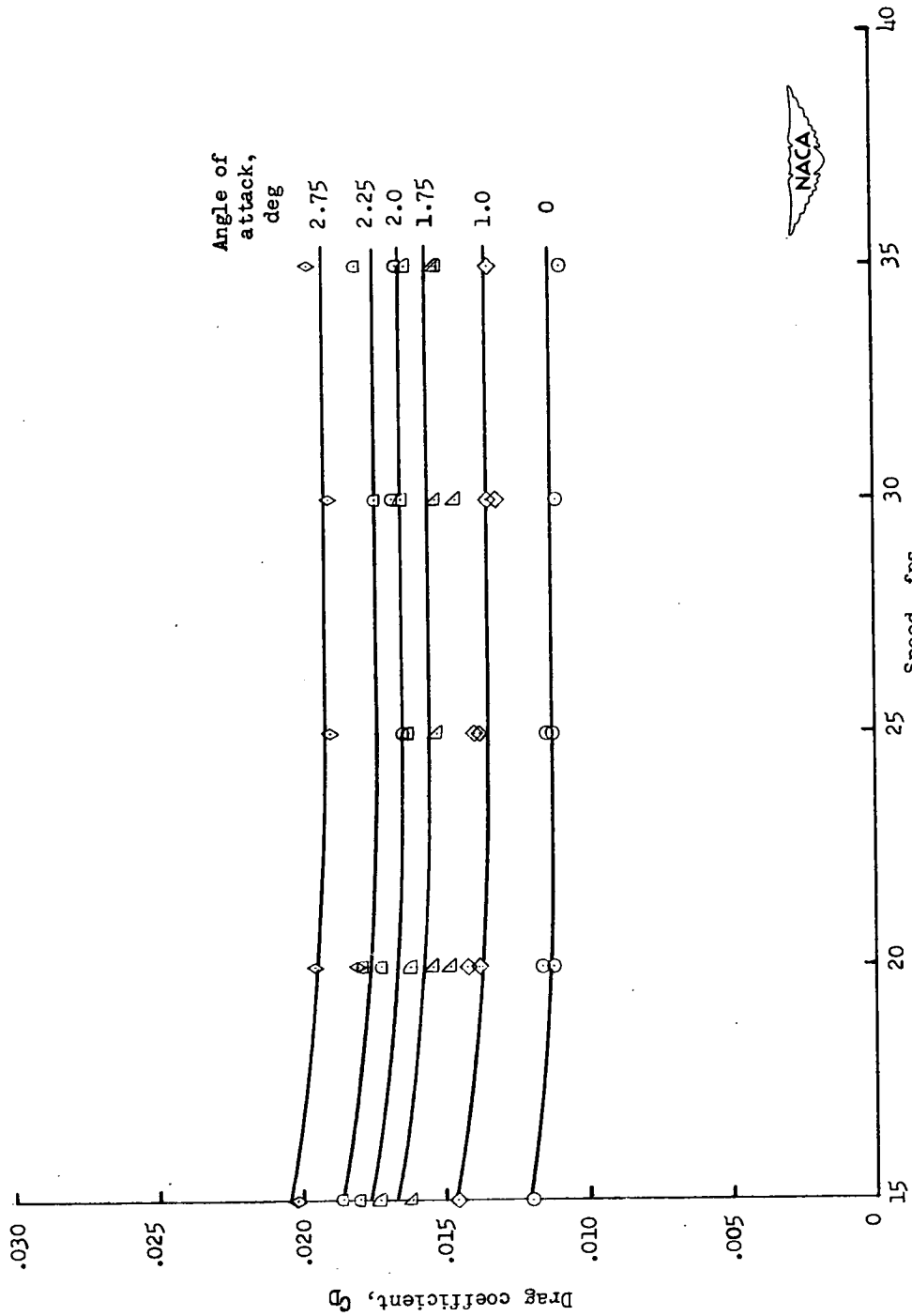

(c) 12.0-inch depth.

Figure 6.- Continued.

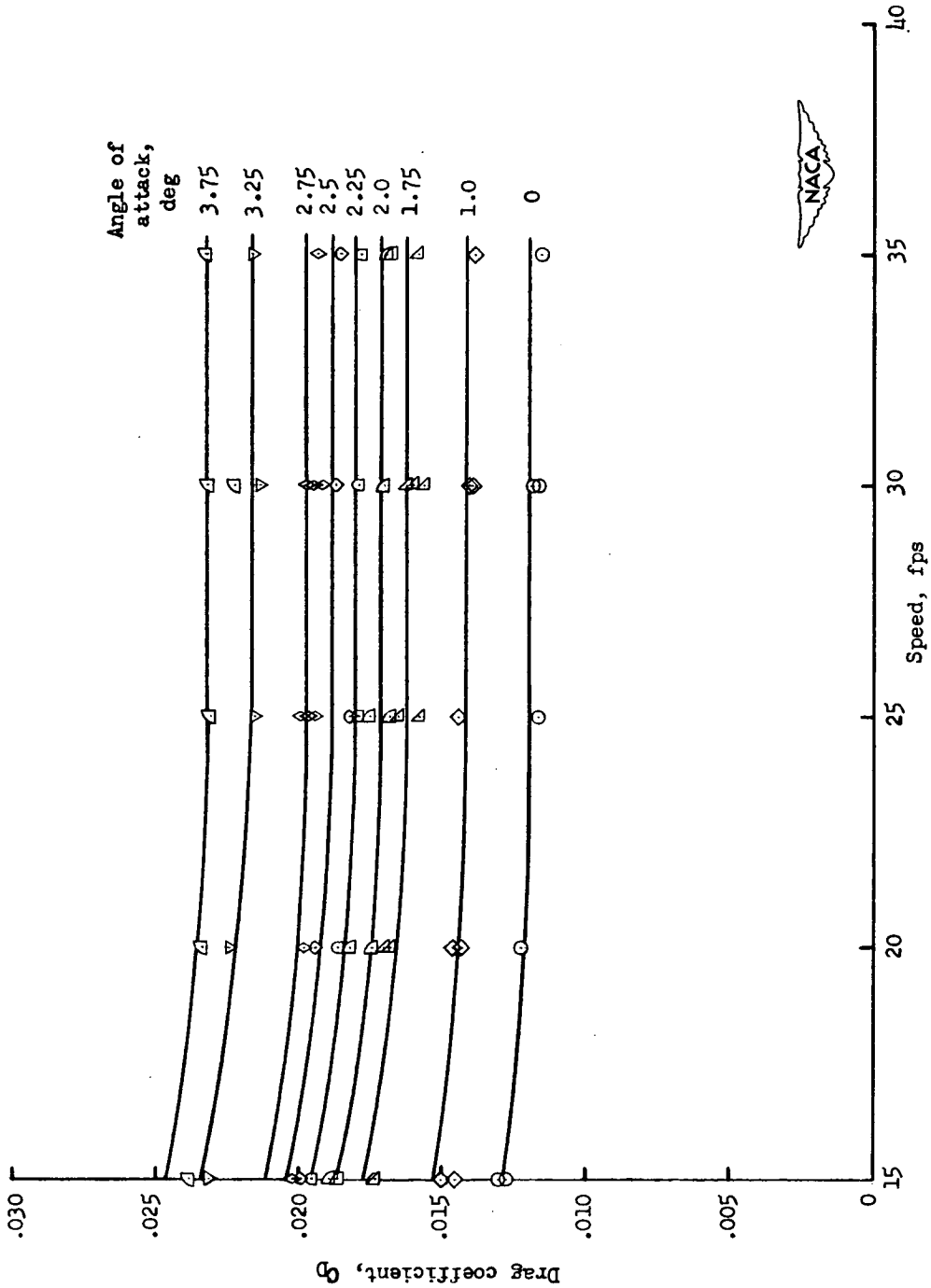

(d) 18.0-inch depth.

Figure 6.- Continued.

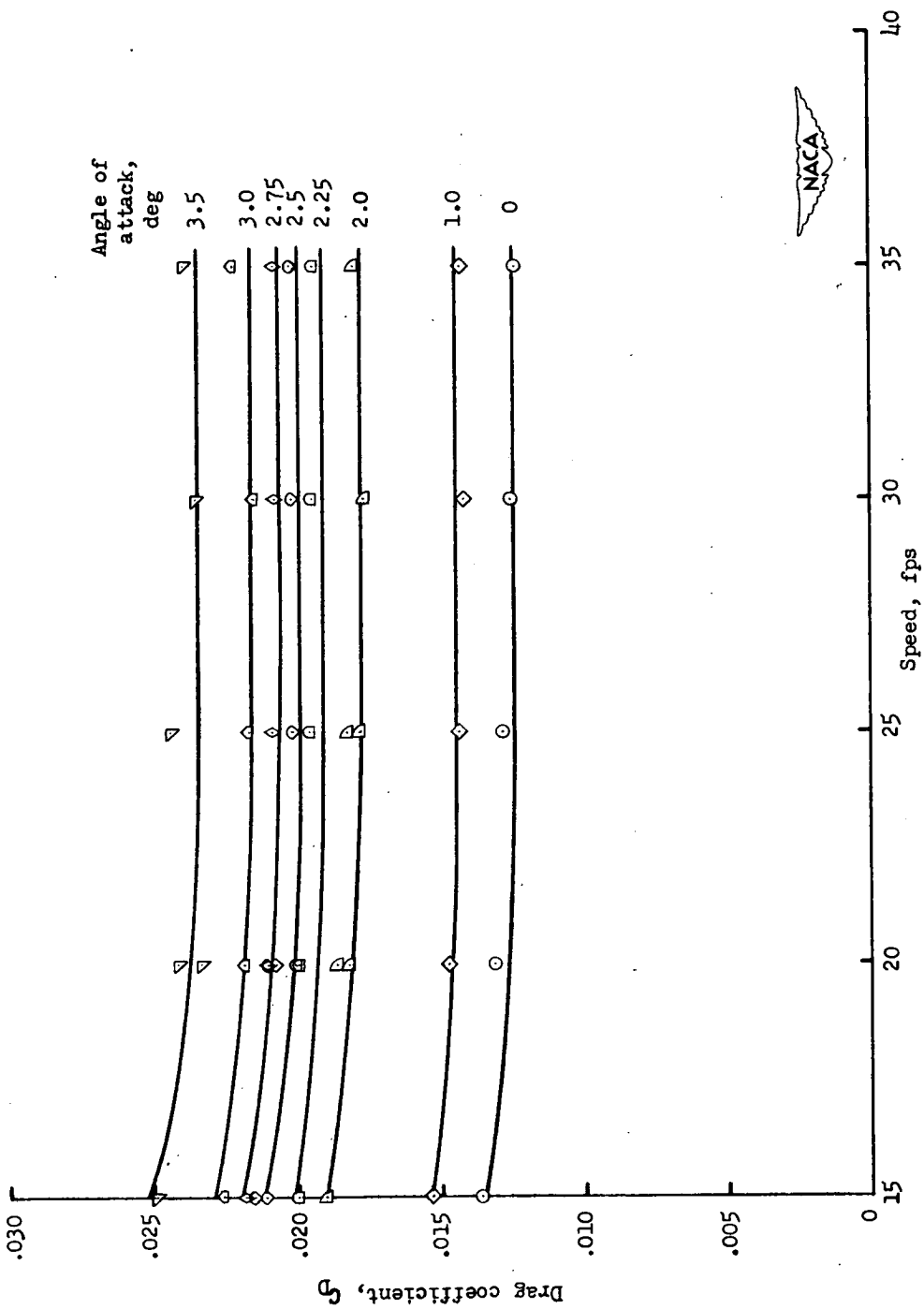

(e) 24.0-inch depth.

Figure 6.- Continued.

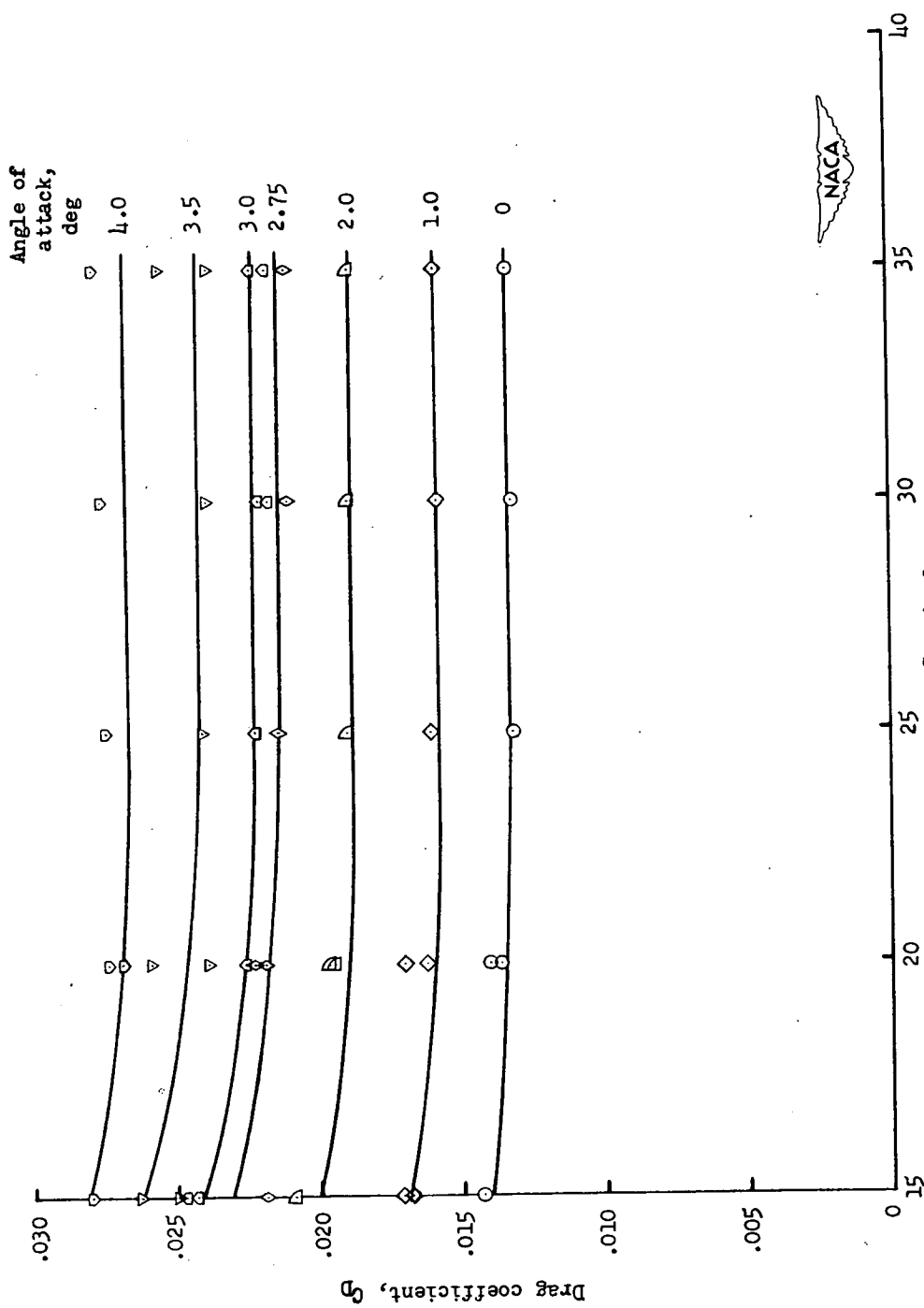

(f) 30.0-inch depth.

Figure 6.- Concluded.

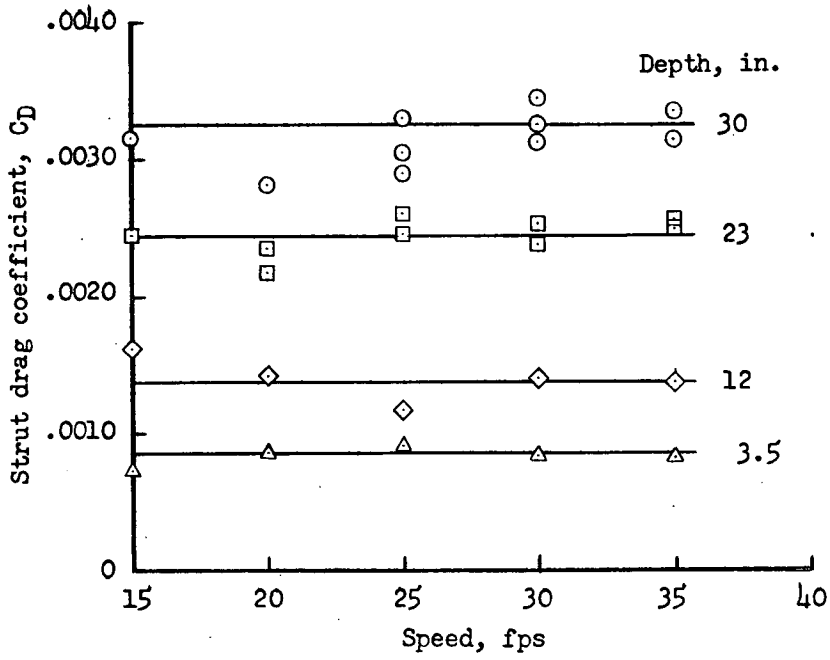

(a) Variation with speed.

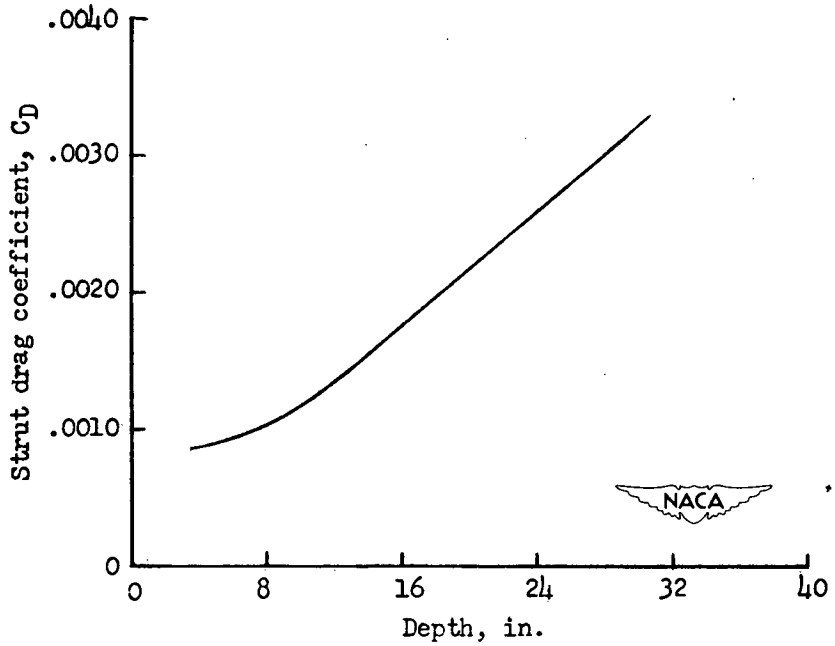

(b) Variation with depth.

Figure 7. - Variation of strut drag coefficient with speed and depth. C_D is based on the area of the hydrofoil (4.44 sq ft).

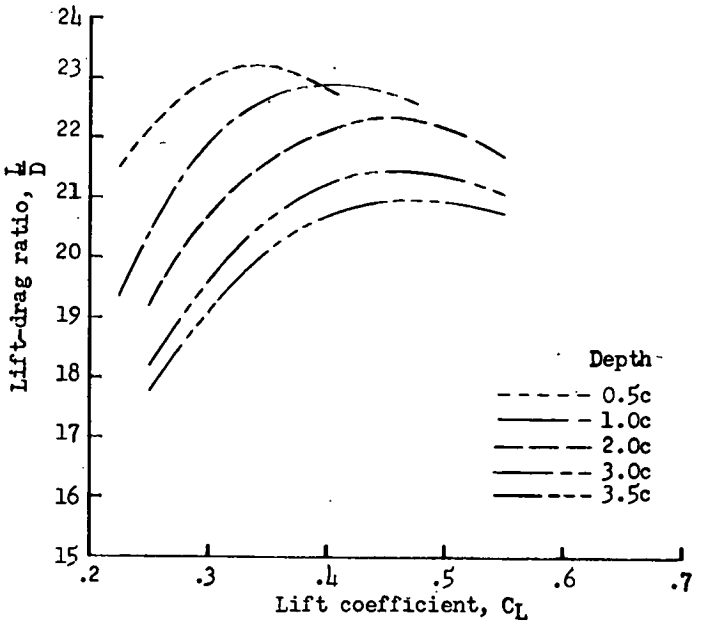

(a) 15 feet per second.

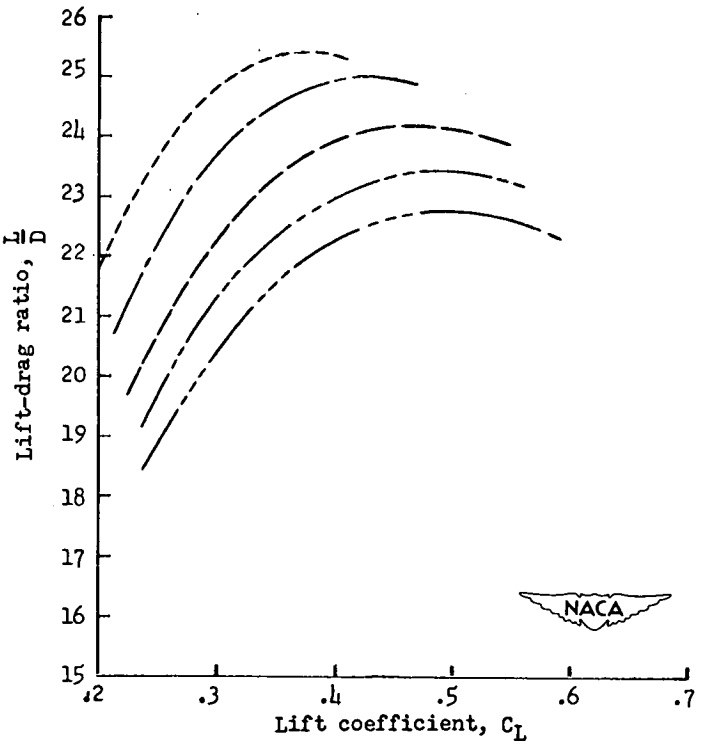

(b) 35 feet per second.

Figure 8.- Variation of lift-drag ratio with lift coefficient and depth of submersion. (Hydrofoil-strut configuration)

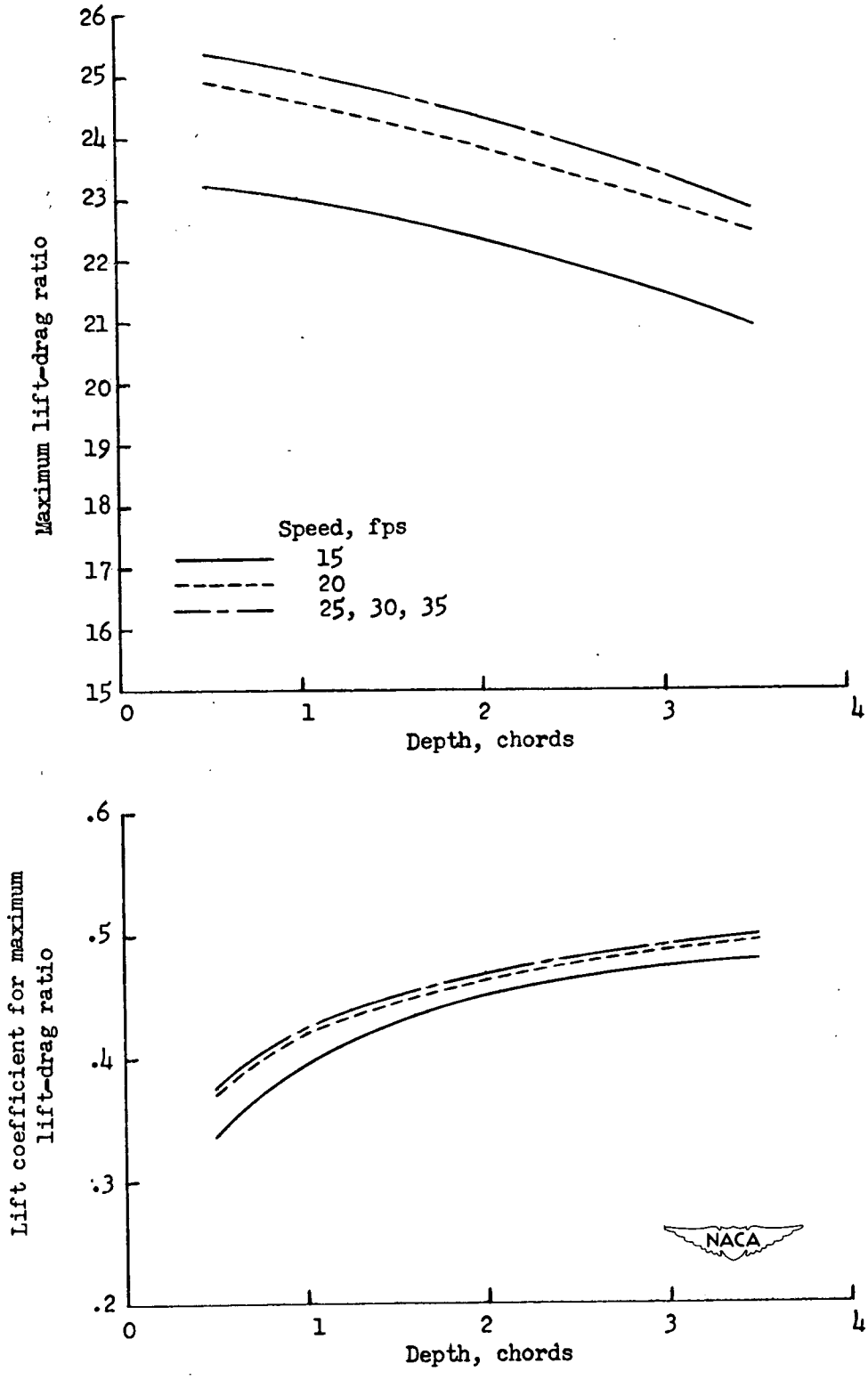

Figure 9.- Maximum lift-drag ratio and the lift coefficient at which it occurs as a function of depth and speed. (Hydrofoil-strut configuration.)

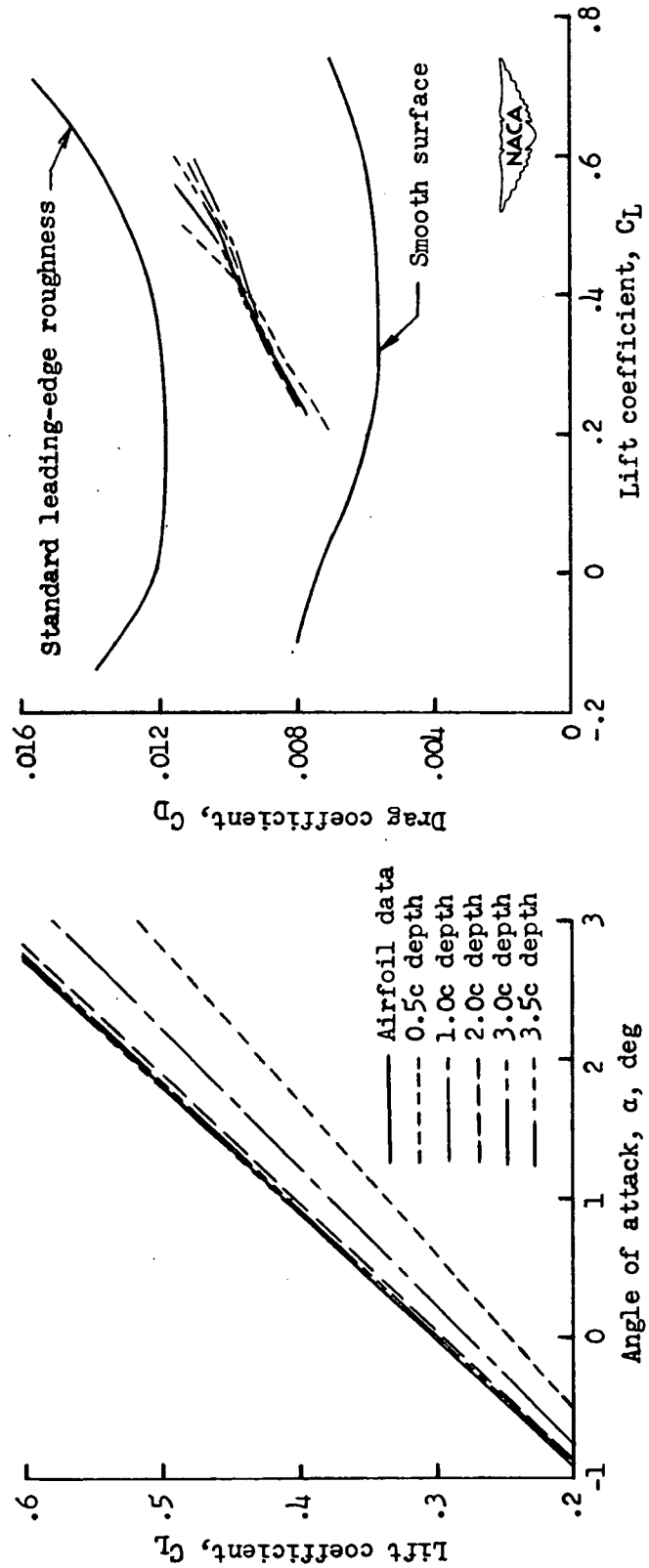

Figure 10.- Lift and drag characteristics of NACA 64_1A412 hydrofoil after corrections for ground effect and aspect ratio compared at a Reynolds number of 2×10^6 with aerodynamic data for the NACA 64_1-412 section.